SAS v5.0 Scientific Validation report (XMM-SOC-USR-TN-0002)

Observation 0122700101 - Revolution 60 - G21.5

M.Guainazzi[1], M.Denby[2], M.Ehle[1], C.Gabriel[1]

[1] *XMM-Newton Science Operation Center, VILSPA, ESA, Apartado 50727, E-28080 Madrid, Spain*
[2] *XMM-Newton Science Survey Center, Department of Physics & Astronomy, University of Leicester, Leicester LE1 7RH, UK*

`15 January 2001`

We report the results of the scientific validation of the XMM-Newton Science Analysis System (SAS) version 5.0 (SASv5 hereinafter), performed on the data of observation nr.**0122700101**. These data belong to the XMM-Newton Performance Verification (PV) phase. They are free from data rights.

The reader is referred to the following URL: `http://xmm.vilspa.esa.es/public/xmm_sas_sv_top.html` for general information about the scope and the procedures of the SAS science validation, and for links to the available documentation on the SAS and the XMM-Newton data format.

1 Purpose of the observation and instrument modes

XMM-Newton observed the region containing the Crab-like SuperNova Remnant (SNR) G21.5-09 (α_{2000}=18^{h}33^{m}33^s.0, δ_{2000}=-10°34'10".0) on April 7 2000, between 12:35:28 and 22:57:20 UTC (revolution number 60). Warwick et al. (2001) have published preliminary scientific results of this observation.

The purpose of including this observation in the SAS science validation process was mainly to:

- check the SAS EPIC response generator functionality
- verify the accuracy of the spectral fitting for the EPIC cameras in the 1–10 keV energy band (G21.5 is absorbed by a column density of $\sim 10^{22}$ cm^{-2}; it is therefore not suitable to check the quality of the spectral fitting in the soft X-rays)
- verify the cross-calibration between the MOS and the p-n cameras in the same energy band

The observation was not affected by high level of radiation (see the MOS1 light curve in the left panel of Fig. 1). The source exhibits a low surface brightness X-ray halo (see the right panel of Fig. 1) within 150" from the SNR

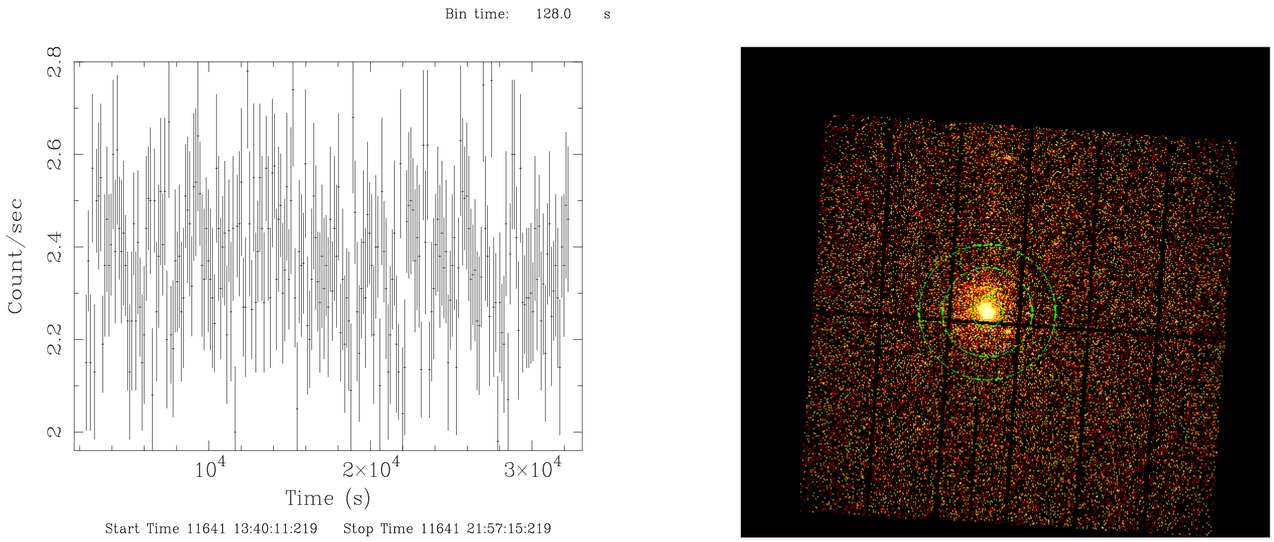

Figure 1: *Left panel*: G21.5 MOS1 light curve in the 0.5–12 keV energy band. The binsize is 128 s. The reduced χ^2, when a constant line is fit to the experimental data is: $\chi^2_\nu = 1.03$. *Right panel*: p-n image in the 0.5-15.0 keV band, showing the extended X-ray halo. The extraction region for the SNR spectrum and the relevant background are shown as *green circles*

centroid.

The instrument modes used in this observation are listed in Tab. 1. OM was not operating.

Instrument	Exposure	Mode	Filter
MOS1	2	Full Frame	Medium
MOS2	3	Full Frame	Medium
p-n	1	Full Frame	Medium
RGS1	4	HER+SES	
RGS2	5	HER+SES	

Table 1: Operational modes used

2 Pipeline products

The reader is referred to Sect. 2 of Guainazzi et al. (2001). In addition to that:

a) the p-n image exhibits a bad column

b) a kind of Moiree pattern is visible in the RGS1 and RGS2 spectral plots, as the 2^{nd} order spectrum is weak and plotted with dashed lines

c) the exposure ID of the ROSAT/XMM-Newton image is 0

d) several spurious sources are detected at the outer upper edge of the p-n chips

Of course, no OM product is present, as OM was not operating during this observation.

3 Functional tests of interactive tasks

Currently, the are three ways for an XMM-Newton user to "produce" EPIC camera response matrices:

1. create a redistribution file with the SAS task `rmfgen` and an ancillary file (*i.e.*: effective area vector) with the SAS task `arfgen`, using the redistribution file created by `rmfgen` as an input
2. create an ancillary file with the SAS task `arfgen`, using a "standard" redistribution file as an input. This option is available for the MOS cameras only, as only MOS "standard" redistribution files are available (files `MOS[12]_all.rmf`)
3. use "standard" response matrices (file `mos1_medium_all_qe17_rmf3_tel5_15.rsp` for *both* MOS cameras; file `epn_fs20_sY#_medium.rmf` for the p-n camera, where # = 1,...,9, according to the position of the source centroid in detector coordinates). These files include both the redistribution matrix and the effective area vector. They can be retrieved at the following URL: `http://xmm.vilspa.esa.es/ccf`.

All three methods are available within SASv5.0. The following section deals with a comparison of their performances. Although the quoted accuracies are probably representative of the systematics still affecting the spectral fitting, the user is urged to repeat such tests on her/his observations, to personally evaluate the robustness of her/his scientific results.

3.1 Relative performances of the EPIC response matrices

The "standard" matrices available for EPIC spectral fitting are optimized for an on-axis source, with an extraction region of approximately 1'. Although it is in principle possible to create response matrix corresponding to different extraction region sizes, the forthcoming results refer to a source spectrum extracted under these conditions. Standard data screening criteria have been applied, as in Guainazzi et al. (2001), and namely:

- 0≤`PATTERN`≤12, `FLAG`=0 and `#XMMEA_EM` true, for the MOS data
- `PATTERN`=0 and `#XMMEA_EP` true, for the p-n data

Source spectra have been rebinned in order to have at least 25 counts in each spectral channel, to ensure the applicability of the χ^2 test to the spectral fits. "Bad" channels have been further removed with the command `ignore bad` in XSPEC 11.0. Background spectra have been extracted from an annulus of radii 175" to 265". The fits have been performed in the 0.5–12 keV and 0.5–15 keV energy band, for MOS and p-n respectively. `arfgen` has been run with parameter `--modelee=no`, as the PSF correction is not implemented yet (cf. Saxton & Siddiqui 2000).

The spectra have been fitted with a simple power-law with photoelectric absorption, as no more complex models are required or obvious spectral features left unexplained. The quality of the fits in the 1–10 keV band is indeed excellent in both the MOS and p-n cameras (see Fig. 2). The residual are dominated by the statistical errors, and suggests that any systematic deviation from the best fit model can be conservatively estimated within $\pm$10%. However, a clear excess is present in the p-n residuals below 1 keV. This excess does not substantially affect the

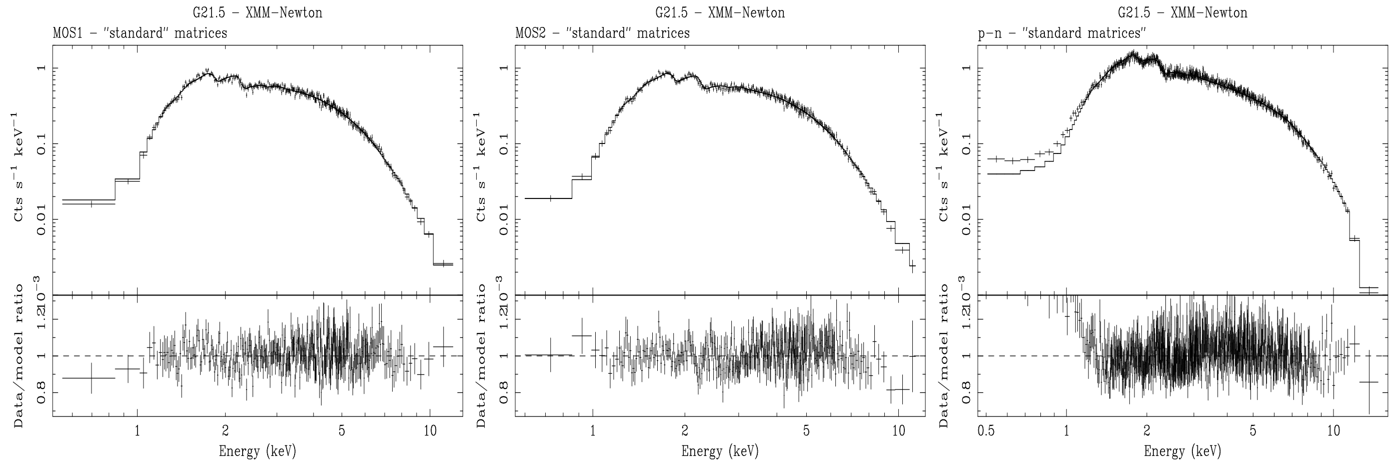

Figure 2: Spectra *upper panels* and residuals in data/model ratio ($\pm$25%; *lower panels*) when a photoelectrically absorbed power-law model is applied to the G21.5 spectra of MOS1 (*left*), MOS2 (*center*) and p-n (*right*).

best-fit spectral parameters reported below. We remind that G21.5 is strongly suppressed in the softer X-ray energy bandpass, and therefore the data discussed in this report are not the most suitable to assess the quality of the EPIC response matrices below 1 keV. Future SV reports will better deal with this issue.

Tab. 2 lists the best-fit parameters and results for the three response generation methods mentioned above. In

Method	Γ	N_H (10^{22} cm^{-2})	2-10 keV flux (10^{-11} erg s^{-1} cm^{-2})	χ^2/dof
MOS1				
1	1.87 ± 0.03	2.28 ± 0.04	5.54 ± 0.05	501.0/416
2	1.90 ± 0.03	2.35 ± 0.04	5.58 ± 0.05	473.9/416
3	$1.84\pm^{0.02}_{0.03}$	2.23 ± 0.04	$5.42\pm^{0.04}_{0.05}$	446.7/416
MOS2				
1	1.83 ± 0.03	$2.22\pm^{0.03}_{0.04}$	5.66 ± 0.05	533.9/415
2	$1.85\pm^{0.03}_{0.02}$	$2.25\pm^{0.04}_{0.05}$	5.66 ± 0.05	423.6/415
3	$1.81\pm^{0.03}_{0.02}$	$2.15\pm^{0.03}_{0.04}$	$5.34\pm^{0.04}_{0.05}$	439.0/415
p-n				
1	$1.905\pm^{0.020}_{0.019}$	$2.33\pm^{0.03}_{0.04}$	$5.25\pm^{0.04}_{0.03}$	1536.3/1154
3	1.855 ± 0.019	$2.28\pm^{0.03}_{0.04}$	$5.06\pm^{0.04}_{0.03}$	1365.1/1155

Table 2: Best-fit parameters and results when a photoelectrically absorbed power-law model is applied to the G21.5 EPIC spectra. The numbers in the first column refer to the three "response matrix generation methods", as described in Sect. 3 of this report. Errors are at the 90% confidence level for one interesting parameter

summary:

- the best fit quality (or at least comparable to the best in the MOS2 case) is achieved when the "standard matrices" are used
- the spectral indices measured in the same instrument agree within $\simeq$3% (typical statistical error $\simeq$1.5%)

- the column densities measured in the same instrument agree within 5% and 2% in the MOS and p-n cameras, respectively (typical statistical error ≃2%)
- the fluxes measured in the same instrument agree within 3%, 6% and 4% for the MOS1, MOS2 and p-n, respectively (typical statistical error ≃1%)

3.2 Off-axis performances and PATTERN dependence

Saxton & Siddiqui (2000) have performed a comprehensive study of the performances of the EPIC response generation task at the time of the SASv5.0 release. Their study includes a wide range of tests on the off-axis and PATTERN dependence of the response matrices, and an estimate of the PSF correction due to photon loss beyond the spectrum extraction radius. Their conclusions can be summarized as follows:

- extracting spectra from MOS events with PATTERN 0 only (which may be appropriate for sources affected by pile-up) induces a negligible steepening of the measured spectral index and a decrease by ≤6% of the measured flux
- spectral fits of sources in an off-axis position produce consistent results to the on-axis case in the MOS cameras and a 3% to 5% steeper spectrum in the p-n
- the PSF correction factors at 20" (67") is 0.72 (1.07)

Saxton & Siddiqui (2000) extend part of the analysis included in this report to further sources, and provide handy recipes to deal with some practical cases (off-axis, pile-up, extended source).

4 Spectral fitting cross-correlation between the EPIC cameras

The G21.5 observation can provide a first glimpse on the spectral cross-correlation among the EPIC cameras. In what follows we refer to the spectral fitting performed with the "standard matrices". In this Section, all confidence levels are for two interesting parameters. In Fig. 3 we compare the iso-χ^2 contour plots for the column density versus

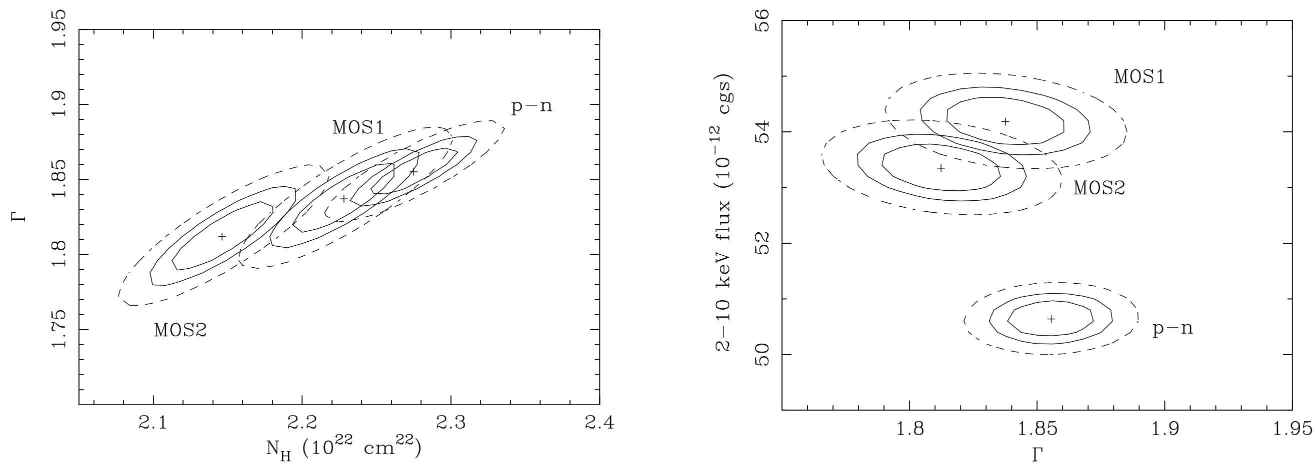

Figure 3: *Left panel*: iso-χ^2 N_H versus Γ contour plot. Lines are at 68%, 90% (*solid lines*) and 99% (*dashed lines*) confidence level for two interesting parameters. *Right panel*: the same for the Γ versus 2–10 keV flux contours

the power-law spectral index (left panel) and the spectral index versus the 2–10 keV flux. We note that:

- spectral indices are consistent if we consider their 99% confidence intervals. (90% between the MOS cameras). The p-n face value is 1% higher than MOS1, which is in turn 1% higher than MOS2
- column densities are well consistent between MOS1 and p-n if we consider their 90% confidence intervals. They are, however, only marginally consistent between the two MOS cameras. The MOS1 face value differ by 4% from the MOS2 and 2% from the p-n one
- MOS best-fit flux values are well in agreement within their 99% confidence interval (the MOS1 being 1% higher). The p-n value is, however, 6% lower than the MOS ones

Acknowledgments

We acknowledge useful comments from R.Saxton and H.Siddiqui - authors of the EPIC response matrix generation SAS tasks - and from C.Erd.

References

M.Guainazzi et al., 2001, XMM-SOC-USR-TN-0001 (*SASv5.0 Scientific Validation Report on the Lockman Hole data*) (available at `http://xmm.vilspa.esa.es/docs/documents/USR-TN-0001-1-0.ps.gz`)
R.D.Saxton & H.Siddiqui, 2000, XMM-SOC-PS-TN-43
(available at `http://xmm.vilspa.esa.es/docs/documents/PS-TN-0043-1-0.ps.gz`)
R.S. Warwick et al., 2001, A&A, 365, L248